

Stepper motors for space applications-ICPE Activities

Mircea Modreanu
ICPE
Senior Scientific Researcher
313 Splaiul Unirii, Bucuresti, Romania
mircea.messico@icpe.ro

Ioana Ionica
ICPE
Scientific Researcher

Cristian Boboc
ICPE
Scientific Researcher

ABSTRACT

The paper presents the development of stepper motors for space applications in ICPE. The approach of these motors has beginning within first ESA contract - Electric Motor Technology Spin Into Space – EMSIS and continued in the second ESA contract, named Stepper Motor for Multimedia Antenna Deployment & Pointing Mechanism of 2nd generation - SM MADPM MKII. The main objective of the first contract is the evaluation of the suitability of ICPE electric motors for the space sector. For the second contract, the main objective is the development of a new version of steppers to address TAS needs for the Multimedia Antenna Pointing Mechanism of 2nd generation (MADPM MKII). The main activities from the projects stages, including design, numerical modeling, manufacturing results from breadboarding stages and experimental results from EM test campaign will be detailed. ICPE, a well-established manufacturer of electric motors at an international level, is in an entering position on this new market through harmonization of the existing electric motor technology with the standard required for the space applications.

KEYWORDS: stepper motor, space applications, numerical modeling, FEM analysis

NOMENCLATURE

BB – Breadboard	PM – Permanent Magnet
EM – Engineering Model	SM – Stepper Motor
H – Hybrid	T _D – Detent Torque
ID – Inner Diameter	T _H – Holding Torque
LEO – Low Earth Orbit	T _L – On load Torque
GEO – Geostationary Orbit	TV – Thermal Vacuum
MDE – Motor Drive Electronics	VR – Variable Reluctance
OD – Outer Diameter	

1 INTRODUCTION

The development of stepper motors (SMs) for space applications in ICPE has beginning with the Electric Motor Technology Spin Into Space - EMSIS contract with ESA and continue in the second contract, named Stepper Motor for Multimedia Antenna Deployment & Pointing Mechanism of 2nd generation - SM MADPM MKII. The approach towards product development was chose based on a preliminary survey that established the particularities of the market from the electric motors' point of view that leads to chose SM.



1.1 State of the art

A SM is an electromechanical device, which converts electrical pulses into discrete mechanical movements [1]. Its shaft rotates with discrete steps when electric command pulses are applied in a proper sequence. The rotor motion is related to the applied pulses. The direction of the motor shaft rotation depends directly by the sequence of the applied pulses. The rotational speed of the shaft is directly related to the input frequency of the input pulses, and the rotation angle is related to the number of pulses [1].

There are three SM types, based on the type of construction:

- Variable reluctance (VR): this type of SM consists of a soft iron multi-toothed rotor and a wound stator stack. In a VR SM, the rotor turns to a specific angle that minimizes the reluctance between opposite windings in the stator [2]. The primary advantage of VR-SMs is their excellent angular resolution. The primary disadvantage is the low torque [2].
- Permanent magnet (PM): the PM SM is a low cost and low-resolution motor [1]. It is an incremental device driven with discrete commands. It responds to these commands by rotating an output shaft in equal angular steps, one step for each input command [3]. The PM-SMs have PMs added to the motor structure instead of teeth. The rotor is magnetized with alternating north and south poles aligned along a straight line parallel to the rotor shaft. These magnetized rotor poles provide for increased magnetic flux density hence the PM SM exhibits improved torque characteristics when compared with the VR SM [1].
- Hybrid (H): the H SM is designed to provide for better efficiency by combining the best features available on both PM SM and VR SM. With the advantage of excellent performances regarding the step resolution, torque and speed, the price is accordingly sizable. The rotor is multi-toothed, and it contains an axially magnetized concentric magnet around its shaft. The teeth on the rotor provide for an even better path, which guides the magnetic flux to preferred locations in the airgap. This further increases the detent torque (T_D) and holding torque (T_H) characteristics of the motor when compared with both the VR and PM types [4].

SM is utilized as actuator in a spacecraft instrumentation system [5], or to control drum actuators for the SNAP-8 program [6]. Consistently, theoretical and experimental work was devoted to study and compare the SMs with conventional closed-loop positioning systems [7], and deploy the SMs to a variety of applications (for solar panels, antennas, or instrumentation).

1.2 Background

The probability of being selected as a supplier for space applications is strongly dependent on the maturity of the products or services being procured. The market of actuators for the space sector covers a wide range of products and there is a clear need for such mechanism in the industry. ICPE, a well-established manufacturer of electric motors at an international level, is in an entering position on this new market through harmonization of the existing electric motor technology with the standard required for the space applications.

EMSIS is a project, under the Romanian Industry Incentive Scheme (AO/1-7557/), through which ICPE was awarded a contract with ESA for evaluating the suitability of its electric motors for the space sector. The main focus of the project was developing a product for operations in space.

The product applications are directed towards LEO or GEO orbits and these needs were used in establishing the environmental conditions for the electric motor. Mostly, SM is the type of motor preferred by all the companies, in the power range from 1 to 20W. In terms of needs not serviced by the current market, all the answers of the mentioned survey relate to SMs and seems to indicate a need for high T_D , this requirement being another indication towards the use of SMs in keeping orientation (for solar panels, antennas, or instrumentation), where is indicated as preferred a precise position control.

Accordingly to the conclusions of the survey report, in the EMSIS project it was chosen to be developed a PM or a H SM, supplied in a frameless configuration (rotor and stator separately), in order to integrate them in the space mechanism applications.

SM MADPM MKII is a project under the Romanian Industry Incentive Scheme (AO/1-8153) through which ICPE was awarded with a contract with ESA for study and develop a new version of SM for MADPM MKII. The main objective is to develop a product to address Thales Alenia Space needs for the Multimedia Antenna Pointing Mechanism of 2nd generation (MADPM MKII), currently under development through ESA NMS Incentive scheme. In the frame of this proposed work, ICPE has the

opportunity to develop a product needed in the space mechanism market and to start, in this first step, a cooperation with TAS France (TAS-F) Competence Center, one of the well-established suppliers of space mechanisms for his telecom satellites as well as scientific and Earth Observation spacecrafts. According to project plan, the activities for first milestone, SRR, were realized. Thus, the SM requirements specification document was established.

The main constructive and technical characteristics of the motor are: H SM, redundant (nominal and redundant windings shall be wound on the same slots), bi-phase, frame-less, voltage supply (voltage/full step) = $26V \pm 10\%$, step angle = $1,0^\circ$, position accuracy ≤ 4 arc min, winding resistance = $86\Omega \pm 10\%$, speed from 0 to ± 120 steps/s, $T_H \geq 0,38$ Nm, running torque $\geq 0,25$ Nm. Also, from the design stage, the electromagnetic modeling for SM was completed.

2 EMSIS PROJECT – ICPE ACTIVITIES

2.1 Motor requirements

The main characteristics of the motor are divided into three categories:

- Main dimensions which includes: total mass (TBD), stator OD (90mm max.), rotor ID (50mm min.), step angle (1deg) and thickness (30mm max.);
- Mechanical characteristics which includes: for 2-phase//(1 phase ON), Min Net output torque-Running torque (Goal is 0.6Nm), T_D (Goal is 0.1Nm); for 4-phase//(1 phase ON), Net output torque-Running torque (Goal is 0.16Nm), T_D (Goal is 0.1Nm);
- Electrical characteristics which includes: for 2-phase//(1 phase ON), voltage ($26 \pm 10\%$), Max. Peak power (20W), electrical time constant (TBC), no load angular error - peak to peak (4 Max. arcmin); for 4-phase//(1 phase ON), voltage ($26 \pm 20\%$), winding resistance - half phase (TBC), winding inductance (TBC), electrical time constant (TBC) and no load angular error - peak to peak (4 Max. arcmin).

The motor shall have the possibility to be configured in two ways:

- As a 2-phase motor;
- As a 4-phase motor.

The switch from 4 to 2 phases will be made at the connector level.

The main winding configuration is presented in Fig. 1.

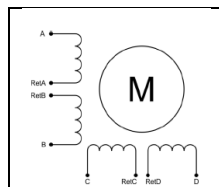


Figure 1: Main winding configuration

The Motor Drive Electronics (MDE) duty cycle is presented in Fig.2.

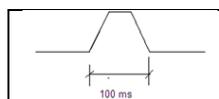


Figure 2: MDE Duty Cycle

Motor Drive Electronics (MDE) characteristics

These electronics are able to drive 2 phases SMs. This is intended for the 2 phases configuration. The motor is driven with following characteristics: Duty cycle from 25% up to 100%, Command frequency < 10 Hz and Supply voltage $26V \pm 10\%$.

2.2 BB process

Having the requirements above, three BB stages and an EM for both motor and drive were considered.

- BB1

In BB1, both PM and H SMs variants were realized. The following materials were used: iron-silicon lamination for the stator and magnetic iron for the rotor, as per ICPE industrial production. In order to optimize the geometry and to obtain the required characteristics according to Specification, numerical modeling based on FEM was largely used.



For the PM SM model, the bi-dimensional models gave accurate results. Due to their construction, this type of SMs can be studied through a bi-dimensional model in a simple planar-parallel problem. Three BBs were manufactured, two with Neodymium – Iron – Boron magnets and one with Samarium-Cobalt PMs. All these BBs did not satisfy all the requirements regarding the winding configuration mentioned in Specification. Therefore, the H SM variant was chosen and for it, is mandatory to use three-dimensional modeling because it has longitudinal magnetization in rotor PM and radial and longitudinal in the stator magnetic circuit.

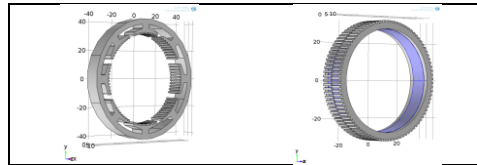


Figure 3: BB1 Constructive elements

For the numerical modeling of the BB1, the following constructive elements were considered: the stator (which has 8 poles with 10 teeth each) and the rotor (which has two semi-armatures with an offset of 2 degrees made of soft iron and a Neodymium – Iron – Boron PM). They are presented in Fig. 3.

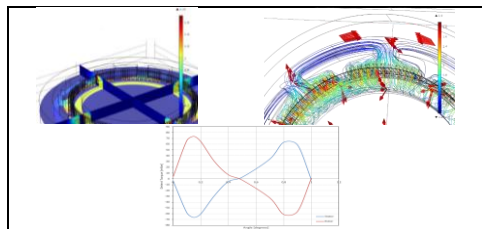


Figure 4: BB1 Numerical modeling results

The postprocessing results for BB1 are presented in Fig. 4. The results are: the color map of the magnetic flux density, the streamlines and arrows for magnetic flux density direction and the calculated T_D – angle characteristic. For T_D computation, the winding is not supplied, so the magnet is the only magnetic source. For numerical modeling, specialized equipment and software based on the finite element method, Comsol Multiphysics, were used. From these results, can be observed that the teeth are charged at airgap where flux concentrators appear. The value of T_D is about 70 mNm.



Figure 5: BB1

BB1 was manufactured and is presented in Fig. 5. The main winding is spread on half of the stator stack and the redundant one is spread on the other half.

- BB2

In BB2, a new version for H SM, different from the material and geometric point of view, was realized.

The following materials were used: iron-cobalt lamination for the stator, magnetic iron for the rotor and Samarium – Cobalt PM. The variant of calculation is in accordance with the overall dimensions of the motor specification, except inner diameter that was increased to 55mm.



Figure 6: BB2 Constructive elements and numerical modeling results



For the numerical modeling of the BB2, the whole magnetic circuit of the motor was considered. It contains the stator and the rotor (has two semi-armatures and one armature, both made of soft iron and two Samarium – Cobalt PMs between them). The postprocessing results for BB2 present the calculated T_D – angle characteristic. The value of T_D is about 90 mNm. They are presented in Fig. 6. For BB2, a numerical model for T_H calculation was developed. Due to the axial symmetry of the motor, only half of the motor was modeled. Because we kept the solution for redundancy from BB1 (the main winding is spread on half of the stator stack and the redundant winding is spread on the other half), for T_H calculation, only half of the main winding which is spread on two poles (half-phase configuration), was considered.

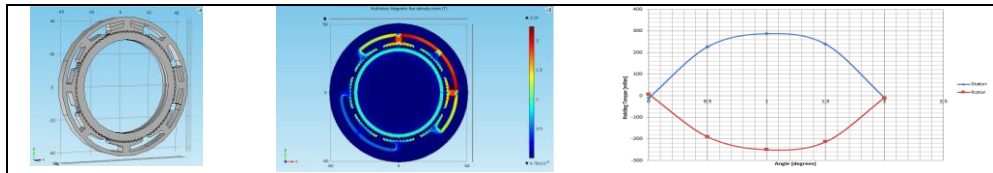


Figure 7: BB2 T_H model

Fig. 7 presents the magnetic circuit and the numerical modeling results for BB2 T_H model. The results are: color map of the magnetic flux density and the calculated T_H – angle characteristic. The maximum value of T_H is about 290 mNm.



Figure 8: BB2

BB2 was manufactured and is presented in Fig. 8. The wound stator stack is only varnished, not embedded.

- BB3 and EM

In BB3 and EM, the redundancy solution was changed. The first solution has some disadvantages, i.e. the use only of half of magnetic circuit and heating of half of motor. The materials used for BB3 and EM remains the same as the ones used in BB2. For BB3, a numerical model for T_H calculation was developed. Due to the axial symmetry of the motor, only half of it was modeled.

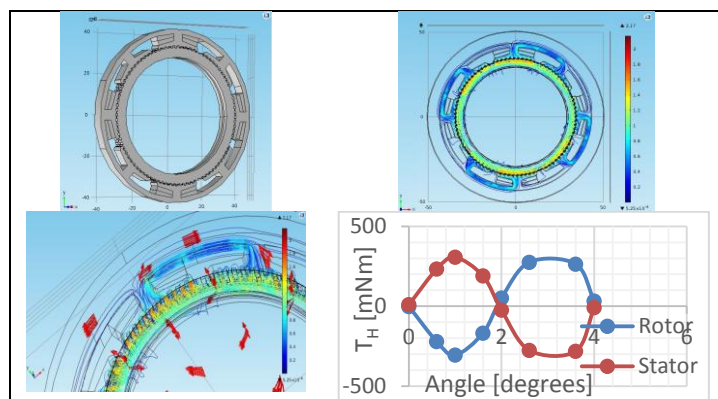


Figure 9: BB3 T_H model

Fig. 9 presents the magnetic circuit with windings and the numerical modeling results for BB3 T_H model, half – phase windings configuration. The results are: streamlines and arrows for magnetic flux density direction and the calculated T_H – angle characteristic. The maximum value of T_H is about 307 mNm.

BB3 and EM were manufactured and they are presented in Fig. 10. The wound stator stack is embedded and on the main and redundant windings thermistors are placed for the motor thermal monitoring.

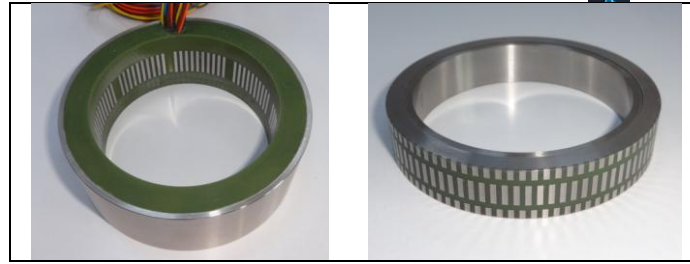


Figure 10: BB3 and EM

2.3 Motor tests

For all BBs and EM, the physical dimensions, the electrical properties and then, the performances of the motor (T_D , T_H and on load torque (T_L)), were measured.

- First measurement method

For BB1, T_D and T_H were measured with a digital dynamometer and the device with the mounted motor fixed on a rotating head, but this method has some disadvantages: difficulty of measurements repeatability and mounting difficulty.

For T_L , a pulley having a known diameter and a measuring masses kit were used. Due to elasticity of the measuring thread, step vibration appears that affects the measurements results.

- Second measurement method

The second measurement method for T_D and T_H uses a torque transducer with angle transducer (with the angle resolution of 1 degree) and the rotor of the motor is rotated with a motoreducer.

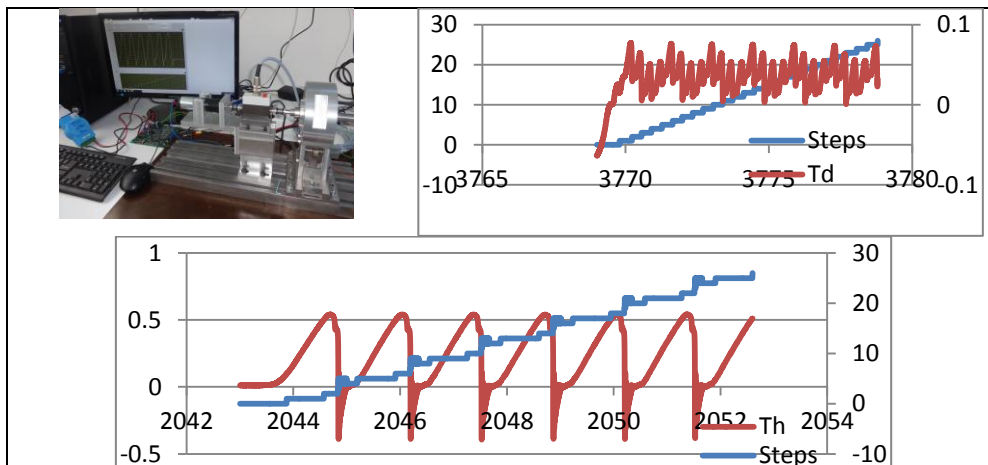


Figure 11: Measurement device and measured diagrams for T_D and T_H

Fig. 11 presents the measurement device and the two measured diagrams for T_D (measured with stator windings unpowered) and T_H – parallel configuration (measured with powered motor - main winding). This method and the measurement device have better results than the previous ones, but have some disadvantages like the impossibility to measure the entire T_H characteristic (the instable part) due to an increased backlash of reducer. This problem will be solved by replacing the actual reducer with another one with 4 arcmin reduce backlash. Another problem of this device are the increased frictions in the slide bearings.

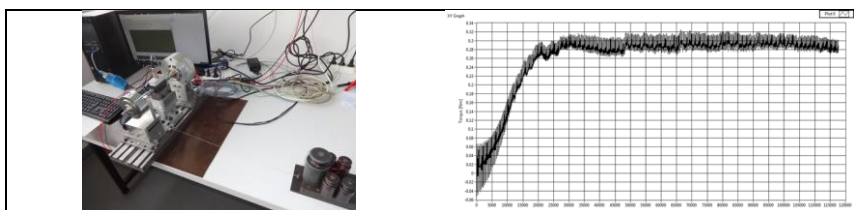


Figure 12: Measurement device and measured diagram for T_L

Fig. 12 presents the measurement device for T_L (measured with powered motor - main winding) and the measured diagram. This device uses a friction load and a torque transducer for T_L measurements.

The presented measurement method has some problems, i.e. T_L is not constant due to a variable friction coefficient and due to difficulty to appreciate the inertia of the load.

- Third measurement method

The previous measurement device for T_D and T_H was improved by replacing the slide bearings with ball bearings having very low friction. This device will be improved by using a reducer with a small backlash.

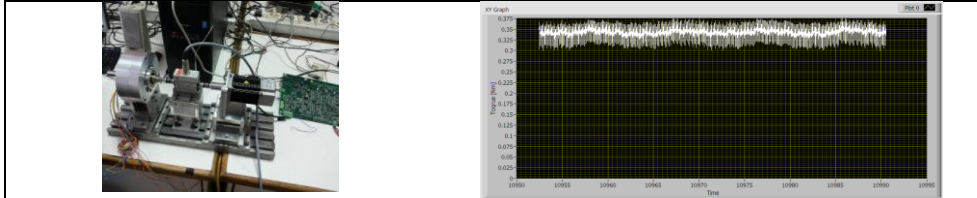


Figure 13: The last measurement device and measured diagram for T_L torque

Fig. 13 presents the last measurement device for T_L (a brushless AC motor controlled in torque, working like a brake) and the measured diagram. This method allows us to measure the pull-in and pull-out torque.

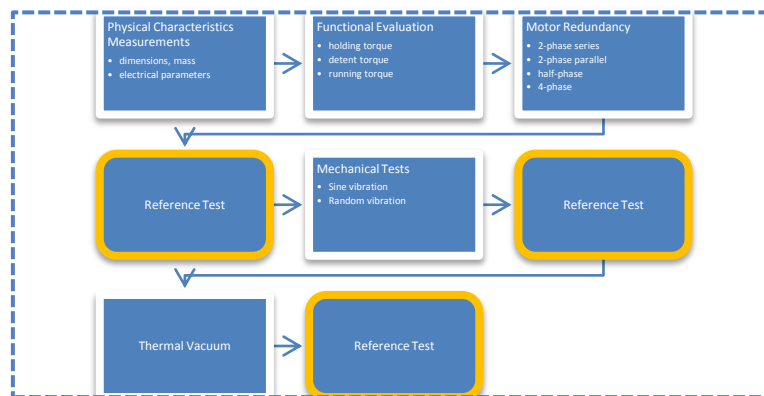


Figure 14: Test flowchart

The last objective of EMSIS project is a test campaign which includes the activity presented in the previous flowchart in Fig. 14. The entire program of EMSIS project was completed, except TV tests on the EM.

3 SM MADPM MKII PROJECT – ICPE ACTIVITIES

3.1 Motor requirements

The main characteristics and the technical requirements of the motor are: H SM, redundant (nominal and redundant windings shall be wound on the same slots), bi-phase, frame-less, voltage supply (voltage/full step) = $26V \pm 10\%$, step angle = $1,0^\circ$, position accuracy ≤ 4 arc min, winding resistance = $86\Omega \pm 10\%$, speed from 0 to ± 120 steps/s, $T_H \geq 0,38Nm$, running torque $\geq 0,25Nm$.

According to project plan, the activities for first milestone, SRR, were realized. Thus, the SM requirements specification document was established.

3.2 BB process

From the design stage, the electromagnetic modeling for H SM according to motor ICD presented in Fig. 15 and to the requirement for minimal stator/rotor airgap (0.1mm), was completed.

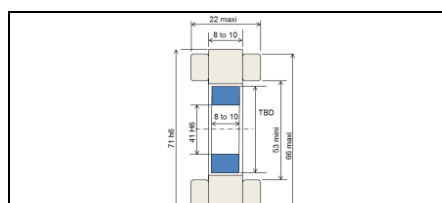


Figure 15: Motor ICD

Till now, five models different from transversal geometry and used materials point of view were considered.

- H SM first model

For the first model, the geometry characteristics are: rectangular teeth both on stator and rotor, tooth width/tooth pitch ratio (t/λ) is 0.5 both on stator and rotor. The following materials were used: iron-cobalt for stator lamination and magnetic iron for rotor semi-armatures.

For numerical modeling of the H SM first model, the following constructive elements were considered: the stator lamination stack (has 8 poles with 10 teeth each) and the rotor (which has two rotor semi-armatures with an offset of 2 degrees and one ring magnet with longitudinal magnetization made of Samarium-Cobalt). The maximum calculated value for T_D is about 14 mNm. In order to optimize the geometry and to obtain the required characteristics according to Specification, FEM based numerical modeling was largely used.

For H SM first model, a numerical model for T_H calculation was developed. This type of problem is formulated in terms of stationary magnetic field. H SM first model has both main and redundant windings spread on the entire stator stack.

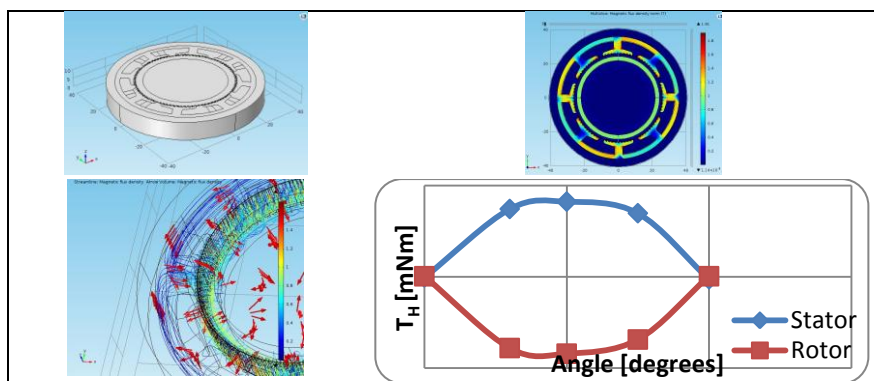


Figure 16: T_H results for H SM first model

Fig. 16 presents the magnetic circuit and T_H numerical modeling results for H SM first model. The results are: the color map of the magnetic flux density, streamlines and arrows for magnetic flux density direction and the calculated T_H – angle characteristic. The maximum calculated value for T_H is about 400 mNm.

Due to the work frequencies (120Hz), that are approximately 10 times bigger than the ones from EMSIS Project and the semi-armatures material which is iron, this variant is not recommended.

- H SM second model

Beginning with the second model, in all H SM models will be used iron-cobalt lamination for the stator and for the rotor semi-armatures. The geometry characteristics are: rectangular teeth both on stator and rotor, tooth width/tooth pitch ratio (t/λ) is 0.5 both on stator and rotor.

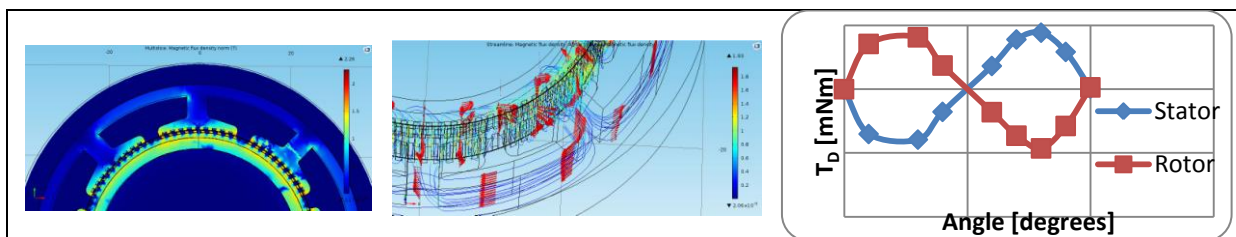


Figure 17: T_D results for H SM second model

The postprocessing results for H SM second model are presented in Fig. 17. The results are: the color map of the magnetic flux density, the streamlines and arrows for magnetic flux density direction and the calculated T_D - angle characteristic. The maximum value for T_D is about 17 mNm.

For H SM second model, a numerical model for T_H calculation was developed. The solution described at H SM first model for main and redundant winding was kept for all models.

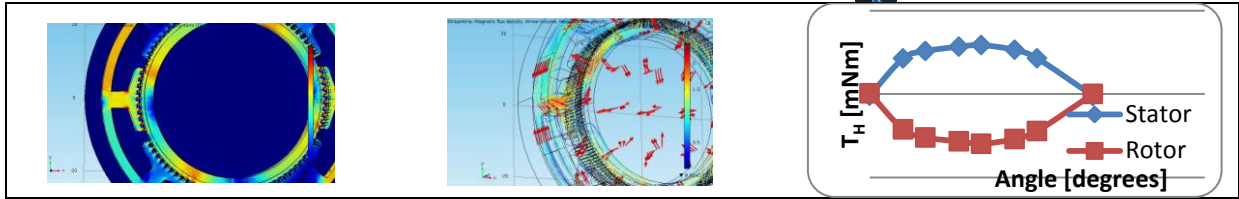


Figure 18: T_H results for H SM second model

Fig. 18 presents T_H numerical modeling results for H SM second model. The results are: the color map of the magnetic flux density, streamlines and arrows for magnetic flux density direction and the calculated T_H – angle characteristic. The maximum value for T_H is about 590 mNm.

- H SM third model

For the third model, the geometry characteristics are: rectangular teeth both on stator and rotor, tooth width/tooth pitch ratio (t/λ) is 0.5 on rotor and 0.38 on stator.

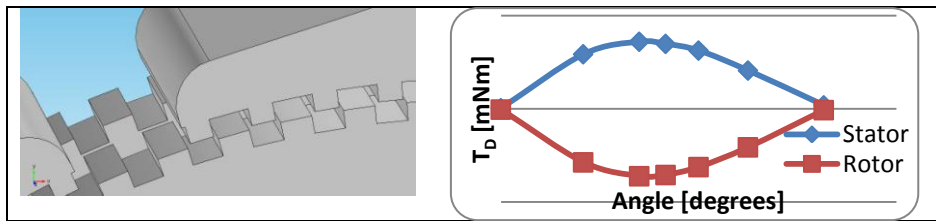


Figure 19: T_D results for H SM third model

Fig. 19 presents the magnetic circuit and the calculated T_D – angle characteristic. The maximum value for T_D is about 36 mNm.

For H SM third model, a numerical model for T_H calculation was developed.

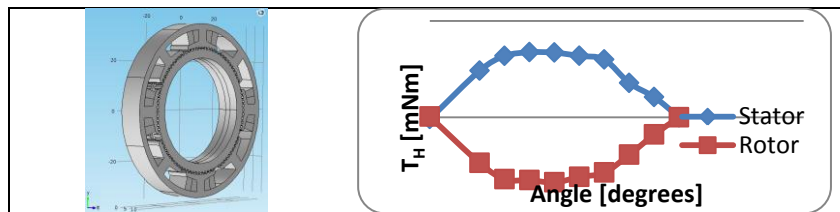


Figure 20: T_H results for H SM third model

Fig. 20 presents the magnetic circuit and the calculated T_H – angle characteristic. The maximum value for T_H is about 670 mNm.

- H SM fourth model

For the fourth model, the geometry characteristics are: rectangular teeth both on stator and rotor, tooth width/tooth pitch ratio (t/λ) is 0.4 on rotor and 0.38 on stator.

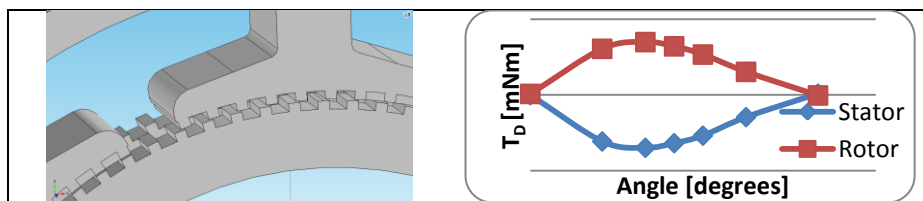


Figure 21: T_D results for H SM fourth model

Fig. 21 presents the magnetic circuit and the calculated T_D – angle characteristic. The maximum value for T_D is about 34 mNm. For H SM fourth model, a numerical model for T_H calculation was developed.

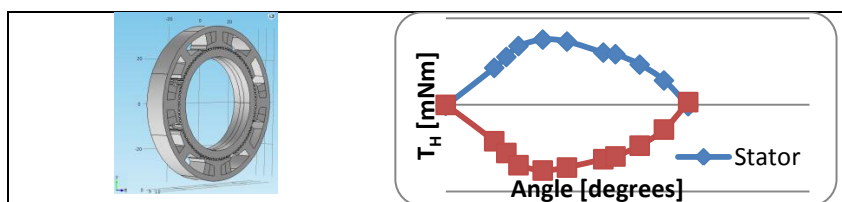


Figure 22: T_H results for H SM fourth model

Fig. 22 presents the magnetic circuit and the calculated T_H – angle characteristic. The maximum value for the T_H is about 760 mNm.

- H SM fifth model

For the fifth model, the geometry characteristics are: trapezoidal teeth both on stator and rotor, tooth width/tooth pitch ratio (t/λ) is 0.4 on rotor and 0.38 on stator.



Figure 23: T_D results for H SM fifth model

Fig. 23 presents the magnetic circuit and the calculated T_D – angle characteristic. The maximum value for T_D is about 32 mNm. For H SM fifth model, a numerical model for T_H calculation was developed.

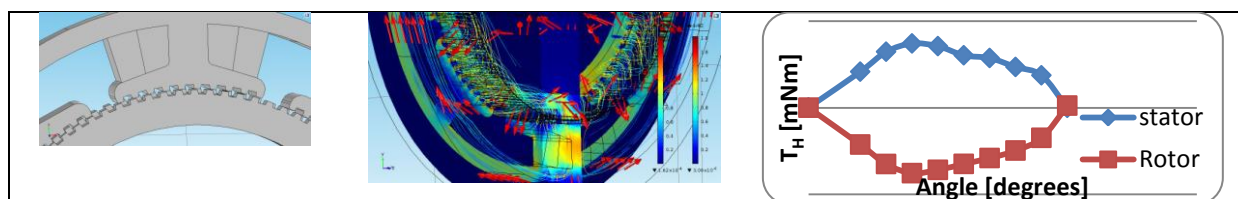


Figure 24: T_H results for H SM fifth model

Fig. 24 presents the magnetic circuit and T_H numerical modeling results for H SM fifth model. The results are: the color map of the magnetic flux density, streamlines and arrows for magnetic flux density direction and the calculated T_H – angle characteristic. The maximum value for T_H is about 740 mNm.

4 CONCLUSIONS

This paper presents ICPE activities in two ESA projects for SM development. The requirements for first project resulted from a survey and for the second project they resulted from TAS needs. The computation results were been highlighted for each studied case. Both project`s activities made possible reaching a TRL 4-5 for SM. More activities are needed, especially in experimental field, in order to bring the SMs manufactured at ICPE on the space market.

REFERENCES

1. L. Bogdan; 2017; "Steppers"; <http://web.ulbsibiu.ro/laurean.bogdan>;
2. M. Scarpino; November 2015; "A Guide to Steppers, Servos, and Other Electrical Machines", 1st ed., Que, pp.59-61;
3. NASA; 2017; <https://ntrs.nasa.gov/archive/nasa/casi.ntrs.nasa.gov/19690011418.pdf>;
4. NMBTC; 2017; <http://www.nmbtc.com/hybrid-step-motors/>;
5. J. C. Nicklas; Jan. 25, 1962; "Analysis, Design and Testing of a Position Servo Utilizing a Stepper Motor". Tech. Rep. 32-206, Jet Propulsion Lab.; California Inst. Tech.
6. S. Giles, A. A. Marcus; Dec. 15, 1964; "SNAP-8-Control-Drum Actuators". Rep. NAA-SR- 9645, Atomics International;
7. S. J. Bailey; *Incremental Servos*. 11, Nov. 1960; "Part I - Stepping vs Stepless Control. Control" *Eng.*, vol. 7, no., pp. 123-127; Dec. 1960; "Part II - Operation and Analysis", vol. 7, no. 12, pp. 97-102; Jan. 1961; "Part III - How They've Been Used", vol. 8, no. 1, pp. 85-88; Mar. 1961; "Part IV - Today's Hardware", vol. 8, no. 3, pp. 133-135; May 1961; "Part V - Interlocking Steppers", vol. 8, no, 5, pp. 116-119;